

UCSF

UC San Francisco Previously Published Works

Title

Brainstem network disruption: A pathway to sudden unexplained death in epilepsy?

Permalink

<https://escholarship.org/uc/item/0881x9j7>

Journal

Human Brain Mapping, 39(12)

ISSN

1065-9471

Authors

Mueller, Susanne G

Nei, Maromi

Bateman, Lisa M

et al.

Publication Date

2018-12-01


DOI

10.1002/hbm.24325

Peer reviewed

RESEARCH ARTICLE

Brainstem network disruption: A pathway to sudden unexplained death in epilepsy?

Susanne G. Mueller¹  | Maromi Nei² | Lisa M. Bateman³ | Robert Knowlton⁴ | Kenneth D. Laxer⁵ | Daniel Friedman⁶ | Orrin Devinsky⁶ | Alica M. Goldman⁷

¹Department of Radiology, University of California, San Francisco, California

²Department of Neurology, Thomas Jefferson University, Philadelphia, Pennsylvania

³Department of Neurology, Columbia University, New York

⁴Department of Neurology, University of California, San Francisco, California

⁵Pacific Epilepsy Program, California Pacific Medical Center, San Francisco, California

⁶Department of Neurology, New York University, New York

⁷Baylor Medical College, Houston, Texas

Correspondence

Susanne Mueller, MD, Center for Imaging of Neurodegenerative Diseases, VAMC San Francisco, 4,150 Clement Street, San Francisco, CA, 94121.

Email: susanne.mueller@ucsf.edu

Funding information

Epilepsy Foundation, Grant/Award Numbers: Epilepsy Foundation grant 325981, 325981; UCSF Resource Allocation Program Award; National Institute of Neurological Disorders and Stroke, Grant/Award Number: U01NS090406-02

Abstract

Observations in witnessed Sudden Unexpected Death in Epilepsy (SUDEP) suggest that a fatal breakdown of the central autonomic control could play a major role in SUDEP. A previous MR study found volume losses in the mesencephalon in focal epilepsy that were more severe and extended into the lower brainstem in two patients who later died of SUDEP. The aims of this study were to demonstrate an association (1) between brainstem volume loss and impaired autonomic control (reduced heart rate variability [HRV]); (2) between brainstem damage and time to SUDEP in patients who later died of SUDEP. Two populations were studied: (1) Autonomic system function population (ASF, 18 patients with focal epilepsy, 11 controls) with HRV measurements and standardized 3 T MR exams. (2) SUDEP population (26 SUDEP epilepsy patients) with clinical MRI 1–10 years before SUDEP. Deformation-based morphometry of the brainstem was used to generate profile similarity maps from the resulting Jacobian determinant maps that were further characterized by graph analysis to identify regions with excessive expansion indicating significant volume loss or atrophy. The total number of regions with excessive expansion in ASF was negatively correlated with HRV ($r = -.37, p = .03$), excessive volume loss in periaqueductal gray/medulla oblongata autonomic nuclei explained most of the HRV associated variation ($r/r^2 = -.82/.67, p < .001$). The total number of regions with excessive expansion in SUDEP was negatively correlated with time to SUDEP ($r = -.39, p = .03$), excessive volume loss in the raphe/medulla oblongata at the obex level explained most of the variation of the time between MRI to SUDEP ($r/r^2 = -.60/.35, p = .001$). Epilepsy is associated with brainstem atrophy that impairs autonomic control and can increase the risk for SUDEP if it expands into the mesencephalon.

KEYWORDS

autonomic control, brainstem, graph analysis, network, SUDEP

1 | INTRODUCTION

Sudden unexpected death in epilepsy (SUDEP) is defined as an unexpected witnessed or unwitnessed death with or without preceding seizure that occurs under benign circumstances in a person suffering from epilepsy. The death is not related to a status epilepticus, drowning or an accident, and autopsy does not provide a cause. SUDEP is the leading cause of death in 10–50% of the patients with chronic drug-resistant epilepsy and is only surpassed by stroke in total potential years of life lost due to a neurological disease (Devinsky, Hesdorffer, Thurman, Lhatoo, & Richerson, 2016; Jones & Thomas, 2017; Thurman, Hesdorffer, & French, 2014; Harden et al., 2017;

Sveinsson, Andersson, Carlsson, & Tomson, 2017). Increased awareness of the SUDEP-related excess mortality in epilepsy patients has led to an intensification of the research efforts to unravel its cause and to the insight that SUDEP is a complex phenomenon that is unlikely to be explained by a single mechanism (Dlouhy, Gehlbach, & Richerson, 2016). The small number of witnessed cases suggests that most patients who succumb to SUDEP are recovering from a severe seizure and are still not fully responsive when it suddenly comes to a breakdown of the autonomic system that is typically initiated by a disturbance of the respiratory function followed by cardiac failure, and often accompanied by a generalized suppression of the EEG activity (Ryvlin et al., 2013). These observations suggest an involvement of

brainstem structures controlling autonomic function (Devinsky et al., 2016), which is also supported by findings in animal models of SUDEP (Holt, Arehart, Hunanyan, Fainberg, & Mikati, 2016). The possible role of brainstem dysfunction in SUDEP was further supported by a MR imaging study demonstrating brainstem volume loss that was most prominent at the level of the dorsal mesencephalon in patients suffering from drug resistant temporal lobe epilepsy. The study population also included two patients who later died of SUDEP in whom the atrophy not only extended from the mesencephalon into the lower brainstem/medulla oblongata but who had also evidence of a structural network disruption that was not seen in the other patients (Mueller, Bateman, & Laxer, 2014). The overall goal of this study was to further probe the potential association between brainstem damage and SUDEP in focal epilepsy. (1) By investigating if atrophy in these regions is associated with reduced heart rate variability (HRV). HRV is a measure of beat-to-beat variability of the heart that results from modulation of the sinoatrial node by the autonomic system and has been shown to be controlled by brainstem structures in neuroimaging studies in humans (Napadow et al., 2008; Sclocco et al., 2016). A reduced HRV has been demonstrated in epilepsy patients and is associated with increased cardiac mortality in nonepilepsy populations (Dlouhy et al., 2015). (2) By demonstrating a more pronounced brainstem volume loss with extension into the medulla oblongata in 26 epilepsy patients who died of SUDEP within 10 years after the MR exam.

2 | METHODS

2.1 | Population

Two different populations were investigated in this project: (1) Autonomic system function (ASF) population. This population consisted of 11 controls (mean age: 30.7 [7.8], m/f: 6/5) and 18 epilepsy patients (mean age: 40.2 [14.1] years, m/f: 9/9) suffering from nonlesional focal epilepsy (temporal and fronto-temporal localization based on semiology and ictal and interictal EEG), please see Table 1. All subjects had been part of a research project conducted at the Center for Imaging of Neurodegenerative Diseases and had undergone a standardized research imaging protocol on the same 3 T magnet. (2) SUDEP population. The population used in this study consisted of a subset of those patients who had been identified as definite or probable SUDEP cases by their treating physicians or medical examiners and been reported to the morphometrics core of the NINDS sponsored Center of SUDEP Research (CSR) who then made every effort to collect all available information and data to be transferred into the CSR data base. At the time of writing, there were 75 cases with MRIs in the data base. The subset investigated in this study consisted of 26 patients (mean age at the last available exam: 22.9 [11.7] years, m/f: 21/5) who had had at least one MR exam acquired for clinical purposes with parameters suitable for quantitative processing (1.5 T or 3 T MRI T1 weighted whole brain image with a resolution of approximately 1.0–1.5 mm × 1.0 to 1.5 × 1–2 mm slice thickness) less than 10 years before SUDEP (please see Table 1 for details). All SUDEP subjects had at least one T1 weighted image fulfilling these criteria, 11 had more than one study from different time points (range 2–7 time points), and 3 had

more than one suitable T1 image acquired with different parameters during the same exam (2–4 images with and without acceleration, different resolution, before and after contrast).

The committee of human research at the University of California, San Francisco (UCSF) and the IRBs of all participating CSR sites had approved the study. Informed consent in accordance with the Declaration from Helsinki had been obtained.

2.2 | Imaging

All ASF subjects were examined as part of a research project that acquired simultaneous EEG recordings on a 3 T Siemens Skyra magnet equipped with a 20 channel receive coil. A T1-weighted gradient echo MRI (MPRAGE) of the entire brain, TR/TE/TI = 2,300/2.96/1,000 ms 1.0 × 1.0 × 1.0 mm³ resolution, acquisition time 5.30 min, was acquired as part of a larger research imaging protocol. The subjects of the SUDEP cohort had undergone MR imaging at 11 different institutions (10 United States, 1 Canada) that used local epilepsy imaging protocols for the exam implemented on magnets of different field strengths and from different vendors (please see Table 1 for details). As all studies were acquired for clinical purposes to be read by local radiologists no efforts had been made to harmonize the imaging protocols (Table 2).

2.3 | Heart rate variability

All subjects in the autonomic study had simultaneous 32 channel EEG including one channel ECG recordings (BRAINAMP MR) during their MR exam. The EEG was set up in a dimly lighted room close to the MR suite and a short baseline EEG (5–10 min) in a relaxed, awake state with eyes closed recorded before the patient was transferred to the MRI for the MR exam. All the exams took place in the mid-afternoon. The ECG obtained during this period was extracted and analyzed with the freely available Kubios HRV (version 2.1) software and heart rate (HR) and heart rate variability (HRV, defined as standard deviation of beat-to-beat intervals) from artifact free sections calculated. The resulting raw HRV was converted into a heart-rate adjusted HRV z-score using the ranges of HR and HRV observed in the control group as initial analyses showed not only the expected dependency of HRV on HR but also a variation of the baseline HR in controls and patients (O'Brien & Dyck, 1995).

2.4 | Image processing and analysis

The heterogeneity of MR platforms and imaging protocols used to acquire the images of the SUDEP cohort prevented the use of standard quantitative image analysis approaches that directly compare imaging features, for example, gray matter volumes derived from tissue segmentation, between a patient group and a control group. The meaningful quantification of these features depends heavily on signal intensity and contrast, that is, requires the use of a standardized and harmonized imaging protocol across groups as was done in the ASF population. A new analysis approach [profile similarity approach (PSI approach, please see below)] that describes the pattern of regional volume loss/atrophy rather than atrophy severity of each region was developed to characterize brainstem atrophy in the SUDEP

TABLE 1 Characteristics of ASF patient population

Patient	Age at MRI	Age at onset	Epilepsy type	Epilepsy syndrome	Lateralization	Localization	MRI	Seizure type
1	52	na	LRE	TLE	R	Temporal	Normal	CPS
2 ^a	22	8	LRE	TLE	L	Temporal	MTS	CPS
3 ^a	54	15	LRE	TLE	R	Temporal	Normal	CPS
4	34	10	LRE	TLE	Bil	Temporal	Normal	SPS,cps
5 ^a	64	na	LRE	TLE	L	Temporal	MTS	SPS
6 ^a	64	60	LRE	TLE	Bil	Fronto-temporal	Normal	CPS
7 ^a	25	Childhood	LRE	TLE	R	Temporal	MTS	CPS
8 ^b	51	28	LRE	TLE	L	Temporal	MTS	SPS, CPS
9 ^b	25	19	LRE	TLE	L	Temporal	Normal	CPS SGTC
10	48	45	LRE	TLE	L	Fronto-temporal	MTS	CPS
11 ^b	29	<1	LRE	TLE	R	Fronto-temporal	MTS	SPS, CPS
12 ^b	27	26	LRE	TLE	R	Temporal	Normal	SPS, CPS
13 ^a	52	na	LRE	TLE	Nonlat	Temporal	Normal	SPS
14 ^a	50	14	LRE	TLE	L	Fronto-temporal	Normal	CPS
15 ^a	27	22	LRE	TLE	R	Temporal	Normal	SPS
16	31	Childhood	LRE	TLE	Nonlat	Temporal	Normal	SPS, CPS
17	39	36	LRE	TLE	Bil	Temporal	Normal	SPS, CPS
18 ^a	29	28	LRE	TLE	L	Temporal	Normal	SPS, CPS

CPS = complex partial; SGTC = secondary generalized tonic clonic; SPS = simple partial; MTS = mesial temporal sclerosis; R = right; bil = bilateral; L = left; nonlat = no lateralizing information in scalp EEC; na = nonavailable.

^aRare seizures (<3/year or SPS only).

^bTherapy refractory epilepsy, evaluation for surgery.

population. The ability of the PSI approach to detect biological meaningful brainstem abnormalities was assessed by comparing its results with those of a standard approach in the ASF population.

2.4.1 | Template generation

Please see Figure 1 for an overview. The template was generated from the T1 images from the 11 ASF controls and from 21 additional healthy controls (add controls, mean age 26.2 [5.9]) who had been studied on the same 3 T MR with the same sequence. Each image was processed in FreeSurfer 5.3 (<http://surfer.nmr.mgh.harvard.edu>). The brainmask and aseg volumes from FreeSurfer were converted into nii. In house written Matlab routines calling SPM imagecalc were used to generate individual brainstem/thalamus/cerebellum masks from aseg. The masks were checked to ensure that the medulla oblongata was consistently covered and manually edited for inaccuracies if necessary before being used to extract the brainstem/thalamus/cerebellum (brainstem plus) from the brainmask volume. The brainstem plus volumes were co-registered (12° affine, fourth degree spline interpolation) to the brainstem plus image of a randomly chosen control subject (target subject) in SPM12. The resulting rbrainstem plus images were used as input for the shoot tool (run shooting, create template, second degree spline interpolation) implemented in SPM12 (Ashburner & Friston, 2011) to generate the brainstem plus template.

2.4.2 | Warping to template and calculation of Jacobian determinants

The images of the remaining subjects (18 ASF patients and 26 SUDEP) were processed in the same way, that is, brainstem/thalamus, cerebellum masks generated from FreeSurfer labels, brainstem plus volumes extracted, and co-registered to the target subject to generate

rbrainstem plus volumes. The rbrainstem plus volumes of all subjects (ASF patients, ASF controls, add controls, SUDEP) were warped onto the brainstem plus template using the shoot tool (run shoot existing templates, Ashburner & Friston, 2011) and the Jacobian determinant maps that summarize the expansions and contractions each image had to undergo during this process calculated. The Jacobian determinants maps were corrected for ICV (as calculated by FreeSurfer), the cerebellum was removed, and nonzero voxels smoothed with a 4 mm FWHM Gaussian kernel using a brainstem only mask. The choice of a 4 mm smoothing kernel was based on experiments in the 3 SUDEP patients in whom more than one T1 weighted image suitable for analysis had been acquired with different parameters, that allowed to study the impact of different acquisition parameters on the measures of interest in the absence of biological changes. For the analysis with the standard approach, the resulting maps were converted into age-corrected z-score maps using the maps from the ASF controls and add controls as reference and the mean intensities for each ROI extracted for analysis (O'Brien & Dyck, 1995). For the analysis with the PSI approach, the corrected and smoothed Jacobian determinants map was used as input.

Brainstem nuclei/regions involved in autonomic control are not distinguishable on a 1.5 or 3 T in vivo image. Ncl ruber, substantia nigra, periaqueductal gray, and a hypointense zone in the ventral pons are faintly outlined which together with the outer brainstem boundaries makes them the main features that drive the template building process and the warping of an individual subject's brainstem onto the template. Volume losses in the brainstem structures of interest, for example, median raphe or reticular formation are indirectly captured if they influence the shape of the outer boundaries or the distance between the faintly depicted internal structures. Therefore macroscopic landmarks identified in the atlas of histological and 9.4 T high

TABLE 2 Characteristics of SUDEP population

Patient	Age at MR	SUDEP type	Time last MR to SUDEP (years)	Epilepsy type	Epilepsy syndrome	Lateralization	Localization	Surgery	No of MR studies	Field strength/magnet type
1	26	Probable	2	CLRE	Undefined	Bilateral	Frontal		2	1.5/Philips
2	17	Definite	3	SLRE	TLE	Left	Temporal	Yes	1	1.5/GE
3	6	Definite	2	SGE	LGS	Bilateral	Multifocal		1	1.5/GE
4	29	Probable	2	LRE	FLE	Undefined	Frontal		1	3.0/GE
5	28	Probable	3	LRE	TLE w MTS	Right	Temporal	Yes	1	3.0/GE
6	25	Probable	5	CLRE	Undefined	Bilateral	Temporal	VNS	2	1.5/Philips
7	45	Definite	3	CLRE	Undefined	Bilateral	Not localized		1	1.5/Philips
8	32	Probable	1	CLRE	Undefined	Bilateral	Multifocal		1	1.5/Philips
9	30	Definite	3	CLRE	Undefined	Bilateral	Temporal		3	1.5/Philips
10	34	Definite	3	CLRE	Undefined	Left	Temporal	Yes	5	1.5/Philips
11	27	Probable	1	CLRE	Undefined	Right	Temporal-parietal	Yes	5	1.5/Philips
12	16	Definite	2	CLRE	Undefined	Left	Occipital	Yes	2	1.5/Philips
13	20	Definite	5	SLRE	Undefined	Bilateral	Multifocal		1	1.5/Siemens
14	1	Definite	1	SGE	Undefined	Bilateral	Bilateral		2	1.5/Siemens
15	1	Probable	1	SGE	Undefined	Bilateral	Bilateral		2	1.5/GE
16	19	Definite	4	CLRE	Undefined	Left	Temporal		1	3.0/Siemens
17	12	Probable	9	CLRE	Undefined	Right	Undefined		1	1.5/GE
18	15	Probable	2	Undefined	Undefined	Undefined	Undefined		1	1.5/GE
19	10	Probable	13	Na	Na	Na	Na		1	
20	21	Probable	5	CLRE	Undefined	Right	Temporal	Yes	3	1.5/Siemens
21	41	Definite	6	CLRE	Undefined	Left	Temporal	Yes	2	1.5/Siemens
22	33	Probable	4	Undefined	Undefined	Bilateral	Bilateral		2	1.5/Siemens
23	24	Probable	5	CLRE	Undefined	Right	Temporal	Yes	4	3.0/Siemens
24	43	Definite	14	CLRE	Undefined	Left	Frontal		1	1.5/Siemens
25	24	Definite	8	LRE	Undefined	Undefined	Undefined		1	1.5/Siemens
26	17	Probable	3	SLRE	Hamartoma	Right	Temporal	Yes	1	3.0/Siemens

LRE = localization related epilepsy; CLRE = cryptogenic localization related epilepsy; SLRE = symptomatic localization related epilepsy; TLE = temporal lobe epilepsy; FLE = frontal lobe epilepsy; MTS = mesio-temporal sclerosis; VNS = vagus nerve stimulator; na = information nonavailable; definite = all criteria for SUDEP met, confirmation by autopsy; probable = all criteria for SUDEP met, no autopsy performed.

resolution sections of the brainstem/medulla (Naidich et al., 2009) were used to identify 67, $5 \times 5 \times 5$ mm large cubic regions of interest (cROIs) that encompassed with a high probability the structures of interest, that is, brainstem structures involved in autonomic control or known to play a role in animal models of SUDEP (e.g., Kommajasyala, Randall, Brozowski, Odintsov, & Faingold, 2017; N'Gouemo & Faingold, 2000; Zhang et al., 2018) (please cf Figure 2 for reference and Supporting Information Figure S3). These 67 cROIs were assigned to 6 system groups based on functional and anatomical properties although it has to be pointed out that all six system groups contained other structures than those after they were named, for example, autonomic nuclei included the caudal part of the reticular formation (cf Supporting Information Figure S3). (1) Autonomic nuclei (19 cROIs in nucleus ambiguus, nucleus of the solitary tract, dorsal motor nucleus of the vagus, hypoglossus, parabrachialis, caudal part of reticular formation). (2) Raphe nuclei or median reticular formation (10 cROIs), (3) Central and lateral reticular formation (18 cROIs), (4) Periaqueductal gray (6 cROIs). (5) Superior/inferior colliculi and ventral tegmentum (8 cROIs), and (6) Tract regions (6 cROIs, medial, lateral lemniscus, medial longitudinal fascicle). System groups 1–5 contain cROIs associated with autonomic control and/or with SUDEP, system group 6 contains major tracts connecting these regions (please see Supporting Information file for co-ordinates).

2.5 | Characterization of the pattern of brainstem deformation by graph analysis: PSI approach

The 67 cROIs were used to extract the mean magnitudes from the ICV corrected Jacobian determinants images of all subjects in the ASF, SUDEP, and add control population. The magnitude of Jacobian determinants is influenced by signal intensity and contrast which means that it does not provide meaningful results in the SUDEP population whose MRI had been acquired with different T1 sequences on different magnets. However, an investigation of the Jacobian determinant maps from those three subjects in whom more than one suitable sequence had been acquired during the same session revealed a remarkably consistent pattern of regions of expansion and contraction despite different absolute magnitudes (cf. Supporting Information Figure S1). Based on this observation, the so-called profile-similarity index (PSI) was developed to characterize the pattern of expansions and contractions captured by the 67 cROIs independently from the magnitude of the Jacobian determinants in the individual Jacobian determinant map. The PSI between cROI_x and cROI_y was defined as follows:

$$\text{rawPSI} = (\text{cROI}_A - \text{mean}_{\text{roi}}) / \text{abs}[(\text{cROI}_x - \text{mean}_{\text{roi}}) - (\text{cROI}_y - \text{mean}_{\text{roi}})]$$

cROI_A is either cROI_x or cROI_y whichever is larger, mean_{roi} , mean over all 67 cROI.

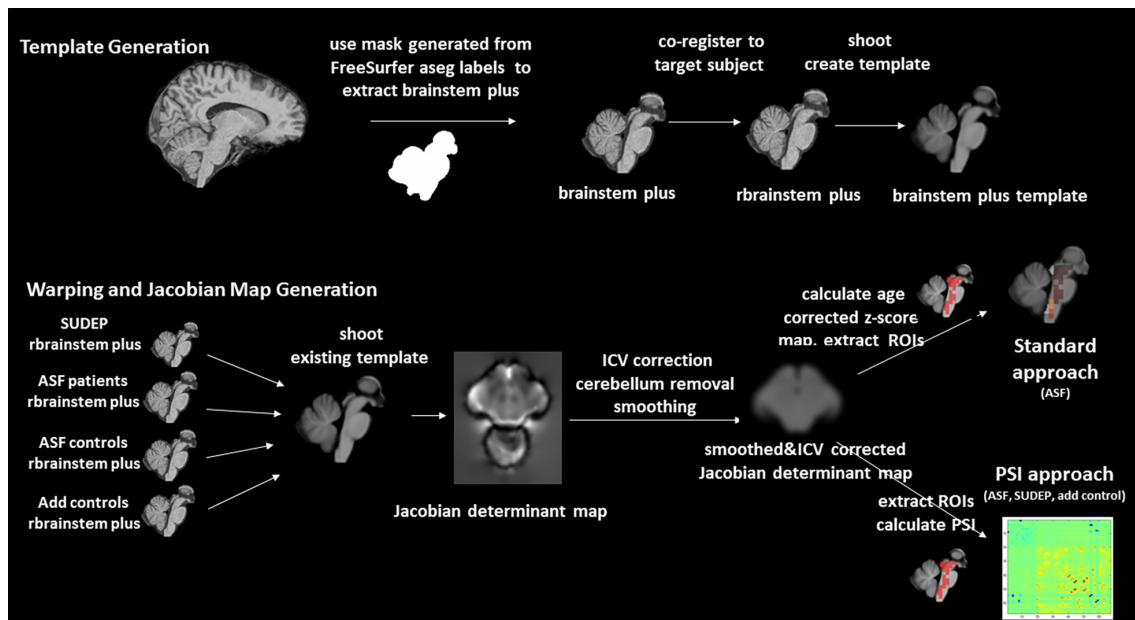


FIGURE 1 Overview of processing pipeline: Upper panel. Template generation. The imaging data from the ASF controls ($n = 11$) and the add controls ($n = 21$) was used for the template generation. Lower panel: Warping and calculation of Jacobian determinant maps [Color figure can be viewed at wileyonlinelibrary.com]

The rawPSI is calculated for each and every combination between two cROIs resulting in a 67×67 matrix of cROIs. The rawPSI values exceeding the 95 percentile of all PSI values in the map are replaced by the PSI value at the 95 percentile to remove outliers caused by a

difference of 0 or very small differences between cROI_x and cROI_y. The rawPSI map is then converted into a the final PSI map by multiplying it with a normalization term n defined as $n = 1/(\text{range of all raw PSI in map})$. A negative PSI indicates an expansion and a positive PSI a

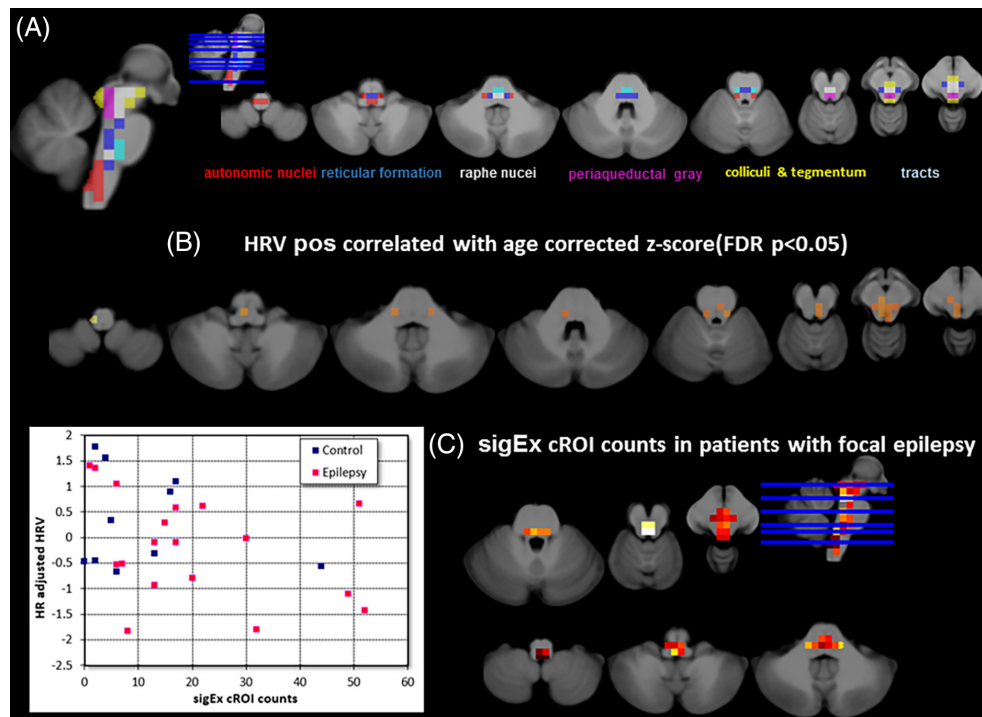


FIGURE 2 The upper panel (a) shows the distribution of the cROIs across the brainstem and their assignment to different systems known to be involved in autonomic control. The middle panel (b) shows the results of the processing with the standard approach. The distribution of cROIs whose mean age-corrected z-scores were significantly ($p < .05$ FDR) correlated with heart rate corrected HRV in the patients of the autonomic group. The lower panel (c) shows the results of the processing with the PSI-based approach. On the left is the scatter plot of the sigEx cROI counts and HRV in patients (red dots) and controls (blue dots) (please see text for correlations) and on the right is the distribution of sigEx cROIs in the patients of the autonomic group. The color indicates the number of patients who had sigEx cROIs in this particular location with bright yellow indicating the highest number ($n = 13$) and dark red the lowest number ($n = 1$). sigEx cROIs with high subject counts were found in the region of periaqueductal gray and the raphe and reticular nuclei but also in some autonomic nuclei [Color figure can be viewed at wileyonlinelibrary.com]

contraction relative to the mean expansion/contraction that had to be applied to the brainstem region covered by the 67 cROIs when warping this individual's brainstem to the template. It is assumed that the PSI map of an individual healthy control is determined by this person's individual anatomical features and thus that the PSI maps of the control group capture the common anatomical brainstem variants. A pathological process within the region covered by the 67 cROIs will introduce additional areas of expansion and/or contraction associated with this process that will change the appearance of the resulting PSI map compared with those of the control group. Graph theory is used to summarize the expansion/contraction pattern captured by each subject's PSI map. The routines provided by the Brain Connectivity Toolbox (<https://sites.google.com/site/bctnet>), in particular the weight conserving measures "strength," diversity and modularity were used for this purpose (Rubinov & Sporns, 2011). Weight conserving measures have the advantage that they can be applied to fully connected networks, that is, it is not necessary to define an arbitrary threshold to generate the type of sparse network required by the more commonly used non weighted equivalents degree and participation coefficient. Strength is defined as the sum of weights of links connected to a node or a cROI. A cROI has a high strength if it has experienced a similar degree of expansion/contraction as the majority of the other cROIs and a low strength if there are only few other cROIs with similar expansion/contraction. A brainstem with a pathological process/lesion will require a more complex pattern of expansions/contractions to be warped onto the template than a normal brainstem. As a consequence, there will be fewer cROIs that experience a similar degree of expansion/contraction as the cROIs within the lesion. This will reduce the strength of the cROIs within the lesion and to a lesser degree also the strength of some cROIs outside the lesion compared with the cROIs from this region in a normal brainstem. Modules are nonoverlapping groups of nodes that are highly interconnected while having comparatively few connections with nodes outside of that group. The number of connections of a node with nodes outside its module is described by diversity. A high diversity indicates that the node has a high number of connections with nodes not belonging to the same module and a low diversity that the node is mostly connected to other nodes belonging to the same module. In the context of a PSI map, cROIs with similar degree of expansion/contraction are likely to be assigned to the same module. The more complex pattern of expansions/contractions that is required to warp a brainstem with a pathological process/lesion onto the template will increase the number of modules and lower the diversity of the cROIs within the lesion and to a lesser degree also in cROIs outside the lesion. Finally, the BCT algorithms for strength and diversity distinguish between positive and negative strength and positive and negative diversity. In the context of the PSI map, the negative strength/diversity of a cROI provides a measure of relative expansion (to compensate for relative volume loss) and the positive strength and diversity a measure for relative contraction (to compensate for relative volume growth). Negative strength and diversity were chosen for the analysis as the focus of this study is on expansion as a surrogate for potential volume loss.

2.6 | Characterization of the pattern of brainstem deformation: Standard approach

To investigate if the PSI-based approach is able to pick up meaningful biological information that is comparable to that obtained with a standard approach, the association between HRV and brainstem expansion/contraction was also probed by extracting the mean z-scores from each of the 67 cROIs from the age corrected z-score maps of all ASF controls and patients.

2.7 | Statistical analysis

The nonparametric bootstrapping algorithm from MATLAB and the bias corrected percentile method (DiCiccio & Efron, 1996) was used to calculate the 99% confidence intervals (CI) of the medians of the negative strength and diversity for each cROI in the control group (11 ASF controls, 21 add controls). cROIs in which negative strength and diversity were both below the lower 99% CI were defined as cROIs with significant expansion (sigExcROI) in individual subjects and their total number counted to obtain an expansion severity score. Pearson correlation coefficients were used (A) to identify cROIs whose age adjusted mean z-scores showed a significant positive correlation with heart-rate adjusted HRV in ASF ($p < .05$, FDR correction for multiple comparisons). (B) to test for a negative correlation between total sigExcROI counts/subject as a measure of accumulated brainstem volume loss and HRV in ASF patients and the whole ASF population, and (C) to test for a negative correlation between total sigExcROI counts/subject as measure of accumulated brainstem volume loss in the last available MR exam before SUDEP and the time to SUDEP (in years) in the SUDEP population. To better understand the relationship between the distribution of the sigExcROIs across the brainstem and HRV and time to SUDEP, Spearman rank correlations between all possible combinations of sigExcROIs in each of the six system groups and HRV and time to SUDEP were calculated and the sigExcROI combination with the highest r^2 identified. In the last step, the same procedure was used to identify which combination of all these regional sigExcROI combinations identified in the previous step shared the largest amount of the variation seen in HRV and time to SUDEP.

3 | RESULTS

3.1 | HRV and brainstem abnormalities

Epilepsy patients had a lower heart rate adjusted HRV than controls [-0.176 (1.014) vs. 0.318 (0.941)] but the difference did not reach significance.

3.1.1 | Standard approach

Although patients' age-adjusted z-scores were generally lower than those in controls, only two cROIs in the region of the colliculi had significantly lower scores in patients compared with controls after FDR correction [-0.55 (0.74) vs. 0.27 (0.54) and -0.54 (0.75) vs. 0.24 (0.52), $p = .001$]. Figure 2b depicts the results of the processing with the standard approach. cROIs showing a significant positive

correlation between age adjusted z-score and HRV; most were located in the region of the autonomic and raphe nuclei.

3.1.2 | PSI-based approach

There was a significant negative correlation between the total count of sigEx cROIs in each subject and the subject's adjusted HRV in the combined patient and control group ($r = -.37, p = .03$) that became a trend ($r = -.36, p = .07$) when the analysis was restricted to the patient group indicating a loss of statistical power in the smaller sample, please see Figure 2c, for their distribution. Figure 3 shows sigEx cROIs sharing the largest amount of the variation with HRV in the patient group for each of the six regions [8 autonomic sig Ex cROIs ($r/r^2 = -.69/.47, p = .001$), 2 reticular sig Ex cROIs ($r/r^2 = -.49/.24, p = .02$), 3 raphe sigEx cROIs ($r/r^2 = -.42/.17, p = .04$), 1 periaqueductal gray sigEx cROI ($r/r^2 = -.49/.24, p = .02$), 1 collicular/tegmental sigEx ROI ($r/r^2 = -.33/.11, p = .08$), and 1 tract sigEx ROI ($r/r^2 = -.50/.25, p = .02$)]. When the thus identified 16 sigEx cROIs were analyzed together, the procedure identified the combined counts from a subset of autonomic and periventricular gray sigEx cROIs as the regions sharing the largest amount of variation with HRV ($r/r^2 = -.82/.67, p < .001$, cf. Figure 3 and Supporting Information Figure S2 for details on structures included).

3.2 | Time to SUDEP and brainstem abnormalities

The mean time between the last available MRI exam to SUDEP in the group of SUDEP patients with at least one suitable T1 image was 4.2 (3.4) years. There was a significant negative correlation between each subject's total sigEx cROI count and time to SUDEP ($r = -.39, p = .03$). Figure 2 shows sigEx cROIs sharing the largest amount of the variation with time to SUDEP in the patient group for each of the

6 regions (2 autonomic sig Ex cROIs ($r/r^2 = -.59/.35, p = .001$), 6 reticular sig Ex cROIs ($r/r^2 = -.44/.19, p = .02$), 3 raphe sigEx cROIs ($r/r^2 = -.47/.22, p = .001$), 3 periaqueductal gray sigEx cROIs ($r/r^2 = -.35/.12, p = .1$), 3 colliculi sigEx cROIs ($r/r^2 = -.42/.18, p = .02$), and 1 tract sigEx cROI ($r/r^2 = -.43/.19, p = .02$), and for the sigEx cROIs from all 18 regions with significant correlations in the regional analysis combined ($r/r^2 = -.60/.35, p = .001$). The latter identified the combined counts from a subset of autonomic (upper medulla at obex level) and raphe (dorsal raphe) sigEx cROIs as the regions sharing the largest amount of variation with time to SUDEP. Please see Figure 3 and Supporting Information Figure S3 for details on structures included (Figure 4).

4 | DISCUSSION

There were two major findings: (1) Volume loss/damage in brainstem regions involved in autonomic control was correlated with reduced HRV in epilepsy patients. This suggests that focal epilepsy could lead to brainstem damage (Mueller et al., 2014) and that this damage has the potential to impair the autonomic control system and thereby to increase the SUDEP risk (Ryvlin et al., 2013). The PSI-analysis approach that focused on relative volume losses in autonomic brainstem regions instead of absolute atrophy found a similar damage pattern and identified abnormalities in regions encompassing autonomic nuclei and the periaqueductal gray as those explaining most of the individual HRV variations in epilepsy patients. This suggests that the PSI image analysis approach provides similar information as the standard approach that requires a standardized protocol implemented on the same magnet. (2) Patients who died of SUDEP had widespread brainstem volume loss in their last MR exam before death. More

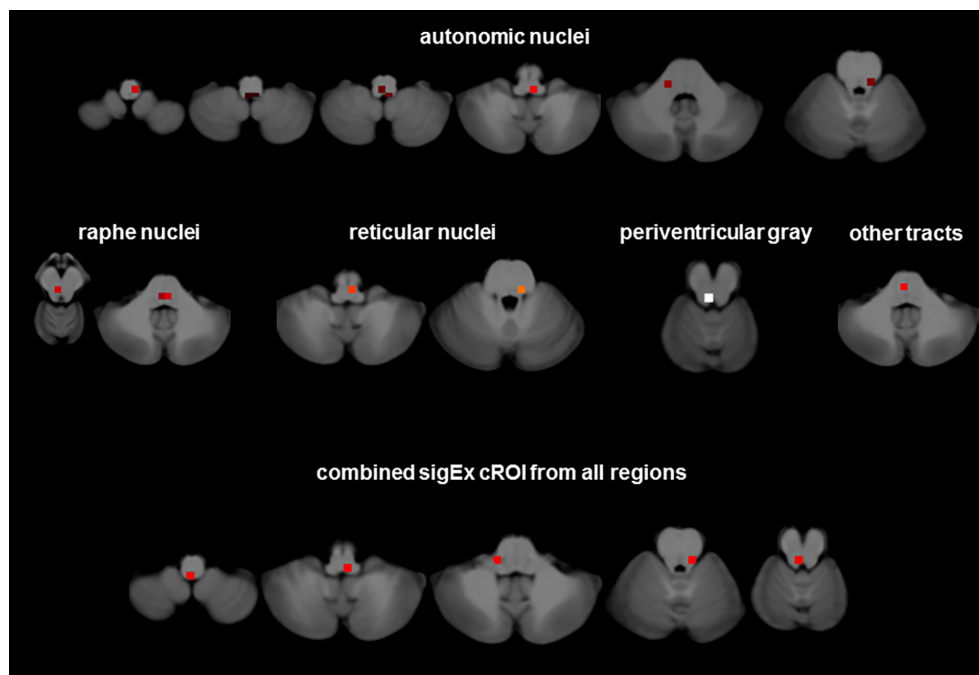


FIGURE 3 sigEx cROIs sharing the largest amount of the variation with heart rate corrected HRV in ASF patients for each of the six regions with significant correlations separately and for the sigEx cROIs from all regions combined. Please refer to the text for r and p values [Color figure can be viewed at wileyonlinelibrary.com]

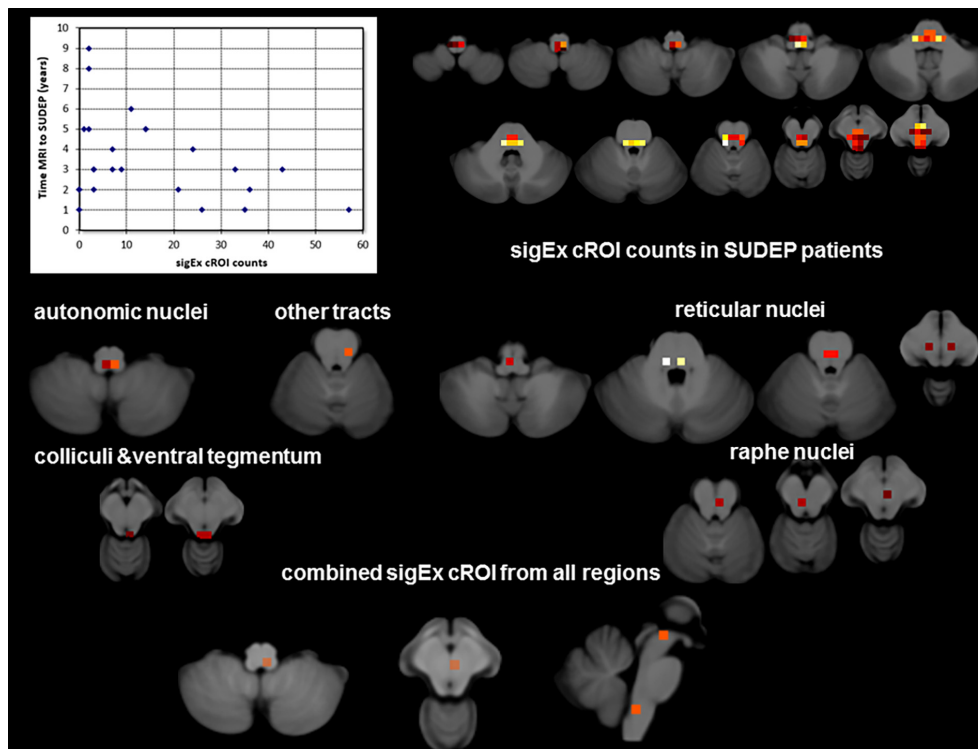


FIGURE 4 The top shows a scatter plot of the sigEx cROI counts and time between last MRI and SUDEP (please see text for correlations) and the distribution of sigEx cROIs in the patients of the SUDEP group the color indicates the number of patients who had sigEx cROIs in this particular location with bright yellow indicating the highest number ($n = 12$) and dark red the lowest number ($n = 1$). The middle and the lower panels show sigEx cROIs sharing the largest amount of the variation with time to SUDEP in the SUDEP population for each of the six regions with significant correlations separately and for the sigEx cROIs from all regions combined. Please refer to the text for r and p values [Color figure can be viewed at wileyonlinelibrary.com]

extensive damage correlated with a shorter survival time. The combined damage in regions encompassing autonomic and raphe nuclei explained most of the variation of time to SUDEP. These observations suggest that focal epilepsy is associated with mesencephalic damage that impairs autonomic control and could increase the risk for SUDEP if it expands into the medulla oblongata and affects nuclei involved in autonomic control. These preliminary findings indicate that it might be possible to detect evidence of this potentially fatal progression of epilepsy associated brainstem damage in MRIs acquired for clinical purposes years before SUDEP.

The results of this study replicate and expand the findings of a previous study that was to our knowledge the first to describe volume loss in the dorsal mesencephalon in patients suffering from temporal lobe epilepsy that extended into the lower brainstem in two patients who died later of SUDEP (Mueller et al., 2014). The previous study used graph analysis to characterize patterns of volume loss in individual patients and found a specific graph analytical signature in the two SUDEP cases indicating an impaired interaction between atrophied regions in the mesencephalon and those in the medulla oblongata (Mueller et al., 2014). The current study confirms these findings by demonstrating similar although less severe volume loss in the region of the colliculi (with FDR correction) and periaqueductal gray (without FDR correction) in a different group of epilepsy patients. These patients were more heterogeneous regarding drug-response compared with the patients in the previous publication who were all undergoing evaluation for epilepsy surgery due to drug resistant

epilepsy. The current study also expands the findings of the previous study by demonstrating a correlation between volume loss in the mesencephalon and autonomic nuclei in the medulla oblongata and reduced HRV. It had not been possible to obtain HRV measurements in the previous study and therefore this finding shows for the first time that MRI detectable volume loss in brainstem regions encompassing autonomic structures provides meaningful information regarding autonomic control even though these structures cannot be distinguished in a standard T1 weighted MR image.

Despite the inability to use a standard image analysis approach due to the heterogeneity of the T1 images in the SUDEP population, the modified approach showed that patients who died of SUDEP had extensive brainstem abnormalities and that their extent was negatively correlated with the time between the last MR exam and death by SUDEP. Furthermore, the results of the individual and combined regional analyses suggest that it was not merely the extent of the brainstem abnormalities but in particular volume loss in the region of the mesencephalon/raphe nuclei and the upper medulla oblongata at the level of the obex that was most highly correlated with the time between last MRI and SUDEP. The latter region corresponds well to the region in which alterations of neuromodulatory, neuropeptidergic, and monoaminergic systems have been shown in a histopathological study of patients who died of SUDEP (Patodia et al., 2018). These findings support the tentative conclusion of the previous study regarding a potential “two-hit” pathomechanism. The two-hit pathomechanism assumes that mechanisms causing structural abnormalities

beyond the focus, for example, excitotoxic effects of spreading seizure activity, are responsible for the mesencephalic abnormalities that represent the "first hit." Dorso-mesencephalic structures, for example, periaqueductal gray, colliculi, raphe, and cuneiform nucleus, not only play an important role in cardio-respiratory control but also in seizure control and arousal (Alvarenga, Pires, & Futuro Neto, 2005; Dampney, 2015; Furman et al., 2015; Müller-Ribeiro, Goodchild, McMullan, Fontes, & Dampney, 2016; N'Gouemo & Faingold, 2000; Soper, Wicker, Kulick, N'Gouemo, & Forcelli, 2016; Trindade-Filho et al., 2008; Zhang et al., 2018). Structural abnormalities in these regions could, therefore, render the patient prone to longer and more severe seizures that are not only more likely to be generalized but also more often associated with prolonged phases of impaired consciousness (Motelow et al., 2015; Zhan et al., 2016; Kundishora et al., 2017) that prevent the patient from perceiving and reacting to a post-ictal respiratory depression. Impaired consciousness is not only observed in witnessed SUDEP cases with preceding seizure but also in those without (Lhatoo et al., 2016) suggesting that it is a crucial factor in the pathomechanism of SUDEP and not just an epiphenomenon of a severe seizure. Prolonged and more severe seizures are not only able to further aggravate the excitotoxic brainstem damage and cause damage in hitherto unaffected brainstem regions but also are more likely to be associated with cardiac arrhythmias and respiratory impairment that in turn could cause additional abnormalities in vulnerable regions, for example, hypoxic damage in the watershed area that encompasses the nucleus of the solitary tract (De Caro, Raffaele De Caro, Parenti, Montisci, & Guidolin, 2000; Jaster et al., 2008; Lorin de la Grandmaison, Paraire, Onaya, & Gray, 2001; Sarnat, 2004). Over time these "second hit" abnormalities will accumulate, structurally and functionally remodel and thereby destabilize the system (Garcia et al., 2016; Kinney, 2009; Villiere et al., 2017; Zanella et al., 2014) until they are severe enough to result in the complete breakdown of the autonomic control in a situation of heightened demand. Although this two-hit scenario is unlikely to be the sole mechanism leading to SUDEP, the fact that it was possible to provide evidence for its existence in two independent patient populations, suggests that it could at least play a role in a subset of patients with focal epilepsy without known genetic risk factors for SUDEP (Anderson, Bos, Cascino, & Ackerman, 2014; Bagnall et al., 2016; Glasscock, Yoo, Chen, Klassen, & Noebels, 2010; Goldman et al., 2009).

To the best of our knowledge, there exists only one other study that used MRI to characterize brain structural abnormalities in SUDEP. Wandschneider et al. (2015) used voxel-based morphometry to compare 12 patients who died of SUDEP and 34 patients with high risk for SUDEP based on previously identified risk factors (frequent convulsive seizures, nocturnal seizures, young age at onset, long duration) with 19 patients with low SUDEP risk but similar epilepsy syndromes and 15 healthy controls. Patients who had died of SUDEP or had a high risk for SUDEP had increased gray matter in the right anterior hippocampus/amygdala compared with low risk patients and controls, which the authors interpreted as a sign for a gliosis or inflammatory reaction in response to repetitive severe seizures that disrupted the autonomic control. The heterogeneous contrast and S/N behavior prevented a VBM analysis in our study's SUDEP population and thus hippocampus and amygdala volumes as provided by FreeSurfer were

used to investigate if the findings of the Wandschneider study could be replicated in this study. This was not the case, (cf. Supporting Information Tables S1 and S2). Although not significant, the SUDEP population had smaller hippocampus and amygdala volumes than the ASF patients who have a low risk for SUDEP by the criteria used by Wandschneider et al. Neither hippocampus nor amygdala volume of the SUDEP group correlated with time from last MRI to SUDEP. However, left and right hippocampal and right amygdala volumes of the ASF population were positively correlated with HRV (cf. Supporting Information data), which is consistent with other reports showing an involvement of hippocampus and amygdala with autonomic control (Napadow et al., 2008). There are several possible explanations for the divergent findings from Wandschneider et al. For example, the standardized imaging protocol used by Wandschneider et al is without doubt better suited to detect subtle differences than the heterogeneous clinical protocol used in our study. Furthermore, the volume increases in the Wandschneider et al. study were restricted to the hippocampal head/amygdala region; hippocampal body and tail volumes were within the normal range. The whole hippocampal volumetry used in our study is less sensitive to regional abnormalities than VBM. This limitation does not apply to the amygdala volumetry though. Finally, the populations in Wandschneider et al. were more heterogeneous regarding MRI visible pathologies, that is, contained patients with normal MRIs and hippocampal sclerosis but also different types of malformations and low grade tumors. There was only one patient with a hamartoma in our SUDEP population. Excluding patients with MRI visible lesions however did not change the findings in Wandschneider et al. indicating that they were not driven by those patients. It has to be emphasized that our inability to replicate the findings of Wandschneider et al., does not exclude an important role of the hippocampus and/or amygdala in our SUDEP population or in SUDEP in general. It does however raise doubts that hippocampal and or amygdala volumes derived from a standard T1 image provide good surrogate measures of that role.

The study has several limitations: (1) Although important, the brainstem is not the only region involved in autonomic control. In addition to hippocampus and amygdala, the mesio-prefrontal regions, parts of the insular cortex thalamus, etc., also play an important role in autonomic control (Cechetto, 2014; Dlouhy et al., 2016; Nagai, Hoshida, & Kario, 2010). Unfortunately, it was not possible to investigate the role of these cortical regions in the SUDEP population because many of the images had either been acquired after contrast injection, surgery or electrode implantation that resulted in artifacts that prevented a reliable thickness measurements. (2) A single ECG trace from the EEG recordings before the MR exam was used for the HRV calculation. Although effective for the purpose of this study, it is not state of the art and it cannot be excluded that more sophisticated ECG recordings would have offered additional insights. (3) The retrospective nature of this study made it necessary to use T1 images from 1.5 and 3 T magnets that had been acquired for clinical purposes. It is not possible to identify the structures of interest reliably on such images making it necessary to use macroscopic features nearby to identify their approximate location. A dedicated high resolution brainstem protocol using multi-modality imaging (T1 in combination with T2 and magnetization transfer weighted images and diffusion tensor

imaging (Lambert, Lutti, Helms, Frackowiak, & Ashburner, 2013; Edlow, MaNab, Witzel, & Kinney, 2015) should be able to resolve at least some of these structures and thus provide a better picture about the exact extent of damage. Such a dedicated protocol is difficult to incorporate into a clinical exam but it should be possible to use the T1 based method described here as a screening tool to identify those patients who might benefit most from the dedicated exam. (4) Finally, the small sample size and the retrospective nature of the study made it difficult to assess the influences of factors such as seizure frequency and types, duration of epilepsy, presumed etiology, etc., on the brainstem findings. The efforts of the morphometrics core and other collaborating entities to identify potential SUDEP cases and collect the relevant data are still ongoing and thus it might be possible to investigate some of these questions in the future.

ACKNOWLEDGMENTS

The authors would like to thank all the relatives of the SUDEP patients who graciously agreed to share the clinical information and MRI images of their loved ones with the CSR Morphometrics Core. They also would like to acknowledge the North American SUDEP Registry (NASR), an independent nonprofit organization that works with families and health care specialists to identify potential SUDEP victims and to collect crucial information and data from those patients that will help to learn more about SUDEP. NASR shared MR images and clinical information from those efforts with the Morphometrics Core. Supported by National Institute of Neurological Disorders and Stroke U01NS090406-02 to AMG and UCSF Resource Allocation Program award and Epilepsy Foundation grant 325981 to SGM.

CONFLICT OF INTEREST

None of the authors has to declare a conflict of interest in relationship to this work.

ORCID

Susanne G. Mueller  <https://orcid.org/0000-0002-5515-4432>

REFERENCES

- Alvarenga, R. M., Pires, J. G., & Futuro Neto, H. A. (2005). Functional mapping of the cardiorespiratory effects of dorsal and median raphe nuclei in the rat. *Brazilian Journal of Medical and Biological Research*, *38*, 1719–1727.
- Anderson, J. H., Bos, J. M., Cascino, G. D., & Ackerman, M. J. (2014). Prevalence and spectrum of electroencephalogram-identified epileptiform activity among patients with long QT syndrome. *Heart Rhythm*, *11*, 53–57.
- Ashburner, J., & Friston, K. J. (2011). Diffeomorphic registration using geodesic shooting and gauss-Newton optimization. *NeuroImage*, *55*, 954–967.
- Bagnall, R. D., Crompton, D. E., Petrovski, S., Lam, L., Cutmore, C., Garry, S. I., ... Semsarian, C. (2016). Exome-based analysis of cardiac arrhythmia, respiratory control, and epilepsy genes in sudden unexpected death in epilepsy. *Annals of Neurology*, *79*, 522–534.
- Cechetto, D. F. (2014). Cortical control of the autonomic nervous system. *Experimental Physiology*, *99*, 326–331.
- Dampney, R. A. (2015). Central mechanisms regulating coordinated cardiovascular and respiratory function during stress and arousal. *American Journal of Physiology. Regulatory, Integrative and Comparative Physiology*, *309*(5), R429–R443.
- De Caro, R., De Caro, R., Parenti, A., Montisci, M., & Guidolin, D. (2000). Solitary tract nuclei in acute heart failure. *Stroke; A Journal of Cerebral Circulation*, *31*, 1187–1193.
- Devinsky, O., Hesdorffer, D. C., Thurman, D. J., Lhatoo, S., & Richerson, G. (2016). Sudden unexpected death in epilepsy: Epidemiology, mechanisms and prevention. *Lancet Neurology*, *15*, 1075–1088.
- DiCiccio, T. J., & Efron, B. (1996). Bootstrap confidence intervals. *Statistical Science*, *11*, 189–228.
- Dlouhy, B. J., Gehlbach, B. K., & Richerson, G. B. (2016). Sudden unexpected death in epilepsy: Basic mechanism and clinical implications for prevention. *Journal of Neurology, Neurosurgery, and Psychiatry*, *87*, 402–413.
- Dlouhy, B. J., Gehlbach, B. K., Kreple, C. J., Kawasaki, H., Oya, H., Buzza, C., ... Richerson, G. B. (2015). Breathing inhibited when seizures spread to the amygdala and upon amygdala stimulation. *Journal of Neuroscience*, *35*, 10281–10289.
- Edlow, B. L., MaNab, J. A., Witzel, T., & Kinney, H. C. (2015). Structural connectome of the human central homeostatic network. *Brain Connectivity*, *2016*(6), 187–200.
- Furman, M., Zhan, Q., McCafferty, C., Lerner, B. A., Motelow, J. E., Meng, J., ... Blumenfeld, H. (2015). Optogenetic stimulation of cholinergic brainstem neurons during focal limbic seizures: Effects on cortical physiology. *Epilepsia*, *56*, e198–e202.
- Garcia, A. J., Zanella, S., Dashevskiy, T., Khan, S. A., Khuu, M. A., Prabkhar, N. R., & Ramirez, J. M. (2016). Chronic intermittent hypoxia alters local respiratory circuit function at the level of the preBötzinger complex. *Frontiers in Neuroscience*, *122*, 831–841.
- Glasscock, E., Yoo, J. W., Chen, T. T., Klassen, T. L., & Noebels, J. L. (2010). Kv1.1 potassium channel deficiency reveals brain-driven cardiac dysfunction as a candidate mechanism for sudden unexplained death in epilepsy. *The Journal of Neuroscience*, *30*, 5167–5175.
- Goldman, A. M., Glasscock, E., Yoo, J., Chen, T. T., Klassen, T. L., & Noebels, J. L. (2009). Arrhythmia in heart and brain: KCNQ1 mutations link epilepsy and sudden unexplained death. *Science Translational Medicine*, *1*, 2ra6.
- Harden, C., Tomson, T., Gloss, D., Buchhalter, J., Cross, J. E., Donner, E., ... Ryvlin, P. (2017). Practice guideline summary: Sudden unexpected death in epilepsy incidence rates and risk factors. *Neurology*, *88*, 1674–1680.
- Holt, R. L., Arehart, E., Hunanyan, A., Fainberg, N. A., & Mikati, M. A. (2016). Pediatric sudden unexpected death in epilepsy: What have we learned from animal and human studies. *Seminars in Pediatric Neurology*, *23*, 127–133.
- Jaster, J. H., Ottavani, G., Matturri, L., Lavezzi, A. M., Zamecnik, J., & Smith, T. W. (2008). Sudden unexpected death related to medullary brain lesion. *The American Journal of Forensic Medicine and Pathology*, *29*, 371–374.
- Jones, L. A., & Thomas, R. H. (2017). Sudden death in epilepsy: Insights from the last 25 years. *Seizure*, *44*, 232–236.
- Kinney, H. C. (2009). Brainstem mechanisms underlying the sudden infant death syndrome: Evidence from human pathologic studies. *Developmental Psychobiology*, *3*, 223–233.
- Kommajosyula, S. P., Randall, M. E., Brozowski, T. J., Odintsov, B. M., & Faingold, C. L. (2017). Specific subcortical structures are activated during seizure-induced death in a model of sudden unexpected death in epilepsy (SUDEP): A manganese-enhanced magnetic resonance imaging study. *Epilepsy Research*, *135*, 87–94.
- Kundishora, A. J., Gummadavelli, A., Ma, C., Liu, M., McCafferty, C., Schiff, N. D., ... Blumenfeld, H. (2017). Restoring conscious arousal during focal limbic seizures with deep brain stimulation. *Cerebral Cortex*, *27*, 1964–1975.
- Lambert, C., Lutti, A., Helms, G., Frackowiak, R., & Ashburner, J. (2013). Multiparametric brainstem segmentation using a modified multivariate mixture of Gaussians. *NeuroImage Clinical*, *2*, 684–694.
- Lhatoo, S. D., Nei, M., Raghavan, M., Sperling, M., Zonjy, B., Lacuey, N., & Devinsky, O. (2016). Non-seizure SUDEP, sudden unexpected death in epilepsy without preceding epileptic seizures. *Epilepsia*, *57*, 1161–1168.

- Lorin de la Grandmaison, G., Paraire, F., Onaya, M., & Gray, F. (2001). Symmetrical necrosis of the solitary tract nuclei as a contributory cause of death. *International Journal of Legal Medicine*, 115, 170–172.
- Motelow, J. E., Li, W., Zhan, Q., Mishra, A., Schdev, R. N. S., Liu, G., ... Blumenfeld, H. (2015). Decreased subcortical cholinergic arousal in focal seizures. *Neuron*, 85, 561–572.
- Mueller, S. G., Bateman, L. M., & Laxer, K. D. (2014). Evidence for brainstem network disruption in temporal lobe epilepsy and sudden unexplained death in epilepsy. *Neuroimage Clinical*, 5, 208–216.
- Müller-Ribeiro, F. C., Goodchild, A. K., McMullan, S., Fontes, M. A., & Dampney, R. A. (2016). Coordinated autonomic and respiratory responses evoked by alerting stimuli: Role of the midbrain colliculi. *Respiratory Physiology & Neurobiology*, 226, 87–93.
- Nagai, M., Hoshida, S., & Kario, K. (2010). The insular cortex and cardiovascular system: A new insight into the brain-heart axis. *Journal of the American Society of Hypertension*, 4, 174–182.
- Naidich, T. P., Duvernoy, H. M., Delman, B. N., Sorensen, A. G., Kollias, S. S., & Haacke, E. M. (2009). Internal architecture of the brainstem with key axial section. In T. P. Naidich, H. M. Duvernoy, B. N. Delman, A. G. Sorensen, S. S. Kollias, & E. M. Haacke, (Eds.), *Duvernoy's atlas of the human brainstem, and cerebellum high-field MRI: Surface anatomy, internal structure, vascularization and 3D sectional anatomy*. Austria, Springer: Vienna.
- Napadow, V., Dhond, R., Conti, G., Makris, N., Brown, E. N., & Barbieri, R. (2008). Brain correlates of autonomic modulation: Combining heart rate variability with fMRI. *NeuroImage*, 42, 169–177.
- N'Gouemo, P., & Faingold, C. L. (2000). Phenytoin administration reveals a differential role of pontine reticular formation and periaqueductal gray neurons in generation of the convulsive behaviors of audiogenic seizures. *Brain Research*, 859, 311–317.
- O'Brien, P. C., & Dyck, P. J. (1995). Procedures for setting normal values. *Neurology*, 45, 17–23.
- Patodia, S., Somani, A., O'Hare, M., Venkateswaran, R., Liu, J., Michalak, Z., ... Thom, M. (2018). The ventrolateral medulla and medullary raphe in sudden unexpected death in epilepsy. *Brain*, 141, 1719–1733. <https://doi.org/10.1093/brain/awy078>
- Rubinov, M., & Sporns, O. (2011). Weight-conserving characterization of complex functional brain networks. *NeuroImage*, 56, 2068–2079.
- Ryvlin, P., Nashef, L., Lhatoo, S. D., Bateman, L. M., Bird, J., Bleasel, A., ... Tomson, T. (2013). Incidence and mechanisms of cardiorespiratory arrests in epilepsy monitoring units (MORTEMUS): A retrospective study. *Lancet Neurology*, 12, 966–977.
- Sarnat, H. B. (2004). Watershed infarcts in the fetal and neonatal brainstem. An aetiology of central hypoventilation, dysphagia, Möbius syndrome and micrognathia. *European Journal of Paediatric Neurology*, 8, 71–87.
- Sclocco, R., Beisser, F., Desbordes, G., Polimeni, J. R., Wald, L. L., Kettner, N. W., ... Barbieri, R. (2016). Neuroimaging brainstem circuitry supporting cardiovagal response to pain: A combined heart rate variability/ultrahigh-field (7T) functional magnetic resonance imaging study. *Philosophical Transactions of The Royal Society A Mathematical Physical and Engineering Sciences*, 374(2067), 20150189.
- Soper, C., Wicker, E., Kulick, C. V., N'Gouemo, P., & Forcelli, P. A. (2016). Optogenetic activation of superior colliculus neurons suppresses seizures originating in diverse brain networks. *Neurobiology of Disease*, 87, 102–115.
- Sveinsson, O., Andersson, T., Carlsson, S., & Tomson, T. (2017). The incidence of SUDEP. A nationwide population-based cohort study. *Neurology*, 89, 1–8.
- Thurman, D. J., Hesdorffer, D. C., & French, J. A. (2014). Sudden unexpected death in epilepsy: Assessing the public health burden. *Epilepsia*, 55, 1479–1485.
- Trindade-Filho, E. M., de Castro-Neto, E. F., de A Carvalho, R., Lima, E., Scorza, F. A., Amado, D., ... Cavalheiro, E. A. (2008). Serotonin depletion effects on the pilocarpine model of epilepsy. *Epilepsy Research*, 82, 194–199.
- Villiere, S. M., Nakase, K., Kollmar, R., Silverman, J., Sundaram, K., & Stewart, M. (2017). Seizure-associated central apnea in a rat model: Evidence for resetting the respiratory rhythm and activation of the diving reflex. *Neurobiology of Disease*, 101, 8–15.
- Wandschneider, B., Koepp, M., Scott, C., Micallef, C., Balestrini, S., Sisodiya, S. M., ... Diehl, B. (2015). Structural imaging biomarkers of sudden unexpected death in epilepsy. *Brain*, 138, 2907–2919.
- Zanella, S., Doi, A., Garcia, A. J., Elsen, F., Kirsch, S., Wei, A. D., & Ramirez, J. M. (2014). When norepinephrine becomes a driver of breathing irregularities: How intermittent hypoxia fundamentally alters the modulatory response of the respiratory network. *Neuroscience*, 34, 36–50.
- Zhan, Q., Buchanan, G. F., Motelow, J. E., Andrews, J., Vitkovskiy, P., Chen, W. C., ... Blumenfeld, H. (2016). Impaired serotonergic brainstem function during and after seizures. *The Journal of Neuroscience*, 36, 2711–2722.
- Zhang, H., Zhao, H., Zeng, C., Van Dort, C., Fangold, C. L., Taylor, N. E., ... Feng, H. J. (2018). Optogenetic activation of 5-HT neurons in the dorsal raphe suppresses seizure-induced respiratory arrest and produces anticonvulsant effect in the DBA/1 mouse SUDEP model. *Neurobiology of Disease*, 110, 47–58.

SUPPORTING INFORMATION

Additional supporting information may be found online in the Supporting Information section at the end of the article.

How to cite this article: Mueller SG, Nei M, Bateman LM, et al. Brainstem network disruption: A pathway to sudden unexplained death in epilepsy? *Hum Brain Mapp*. 2018;39: 4820–4830. <https://doi.org/10.1002/hbm.24325>